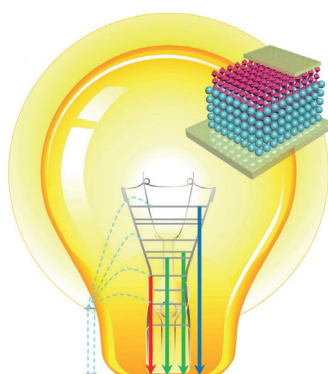


... can greatly accelerate the discovery of new chemical reactions. In their Communication on page 4361 ff., F. Glorius et al. describe a conceptually novel mechanism-based screening approach using luminescence spectroscopy to directly investigate the key quenching step in photocatalysis. As illustrated in the cover image, various photocatalysts and potential substrates undergo “speed dating” with the observation of quenching signifying a promising combination that can be applied in new light-promoted reactions.

Sustainable Polymers

In their Communication on page 4188 ff., E. Y.-X. Chen et al. report the organocatalytic polymerization of γ -butyrolactone to give a high-molecular-weight metal-free polyester with complete recyclability.

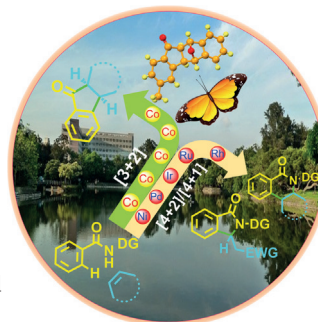


Photovoltaic Devices

In their Communication on page 4280 ff., Z. Lin et al. report a strategy for integrating $\text{NaYF}_4:\text{Yb}/\text{Er}$ upconversion nanoparticles as a mesoporous electrode into organolead halide perovskite solar cells.

C–H Activation

In their Communication on page 4308 ff., C.-H. Cheng et al. describe the diastereoselective synthesis of pentacyclic fluorenones from secondary amides and bicyclic alkenes by cobalt-catalyzed C–H activation.



How to contact us:

Editorial Office:

E-mail: angewandte@wiley-vch.de

Fax: (+49) 62 01–606-331

Telephone: (+49) 62 01–606-315

Reprints, E-Prints, Posters, Calendars:

Carmen Leitner

E-mail: chem-reprints@wiley-vch.de

Fax: (+49) 62 01–606-331

Telephone: (+49) 62 01–606-327

Copyright Permission:

Bettina Loycke

E-mail: rights-and-licences@wiley-vch.de

Fax: (+49) 62 01–606-332

Telephone: (+49) 62 01–606-280

Online Open:

Margitta Schmitt

E-mail: angewandte@wiley-vch.de

Fax: (+49) 62 01–606-331

Telephone: (+49) 62 01–606-315

Subscriptions:

www.wileycustomerhelp.com

Fax: (+49) 62 01–606-184

Telephone: 0800 1800536 (Germany only)
+44(0) 1865476721 (all other countries)

Advertising:

Marion Schulz

E-mail: mschulz@wiley-vch.de

Fax: (+49) 62 01–606-550

Telephone: (+49) 62 01–606-565

Courier Services:

Boschstrasse 12, 69469 Weinheim

Regular Mail:

Postfach 101161, 69451 Weinheim

Angewandte Chemie International Edition is a journal of the Gesellschaft Deutscher Chemiker (GDCh), the largest chemistry-related scientific society in continental Europe. Information on the various activities and services of the GDCh, for example, cheaper subscription to *Angewandte Chemie International Edition*, as well as applications for membership can be found at www.gdch.de or can be requested from GDCh, Postfach 900440, D-60444 Frankfurt am Main, Germany.

GDCh

GESELLSCHAFT
DEUTSCHER CHEMIKER

Get the **Angewandte App**
International Edition



Enjoy Easy Browsing and a New Reading Experience on Your Smartphone or Tablet

- Keep up to date with the latest articles in Early View.
- Download new weekly issues automatically when they are published.
- Read new or favorite articles anytime, anywhere.



Service

Spotlight on Angewandte's Sister Journals

4120 – 4123

Author Profile



*"My favorite food is noodles.
My favorite piece of music is Going Home (Kenny G) ..."*
This and more about Zhenfeng Xi can be found on
page 4124.

Zhenfeng Xi _____ 4124

News



J. S. Siegel



P. J. Stang



M. Antonietti



S. Schlemmer

Friendship Award:
J. S. Siegel and P. J. Stang _____ 4125

International Science and Technology
Cooperation Award: P. J. Stang ____ 4125

Gay-Lussac Humboldt Prize: M. Anto-
nietti and S. Schlemmer _____ 4125

Books

Never Lose Your Nerve

Alan J. Heeger

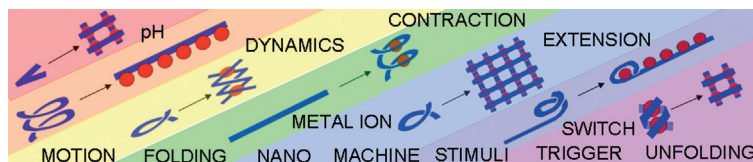
reviewed by G. Wegner* _____ 4126

Reviews

Molecular Motion

M. Barboiu, A.-M. Stadler,
J.-M. Lehn* _____ 4130–4154

Controlled Folding, Motional, and
Constitutional Dynamic Processes of
Polyheterocyclic Molecular Strands



This Review discusses the structural and functional features of polyheterocyclic ligand strands that display designed specific shapes, undergo shape changes on

binding of metal cations, and perform various types of pH-responsive motions induced by metal ions.

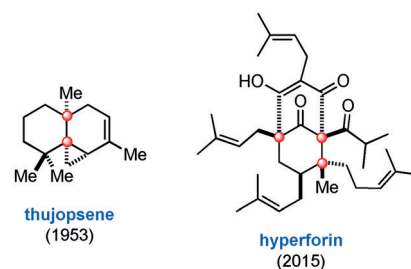
Contiguous Quaternary C Atoms

M. Büschleb, S. Dorich, S. Hanessian,*
D. Tao, K. B. Schenthal,
L. E. Overman* _____ 4156–4186



Synthetic Strategies toward Natural
Products Containing Contiguous
Stereogenic Quaternary Carbon Atoms

Raising the bar: The impressive achievements in the total synthesis of complex natural products containing two or three stereogenic contiguous quaternary carbon centers since 1953 are showcased by many creative strategies. The height of the “synthesis bar” can now be raised to consider hitherto unconquered molecules with multiple contiguous quaternary carbon atoms, each residing on a stereogenic carbon atom.



Communications

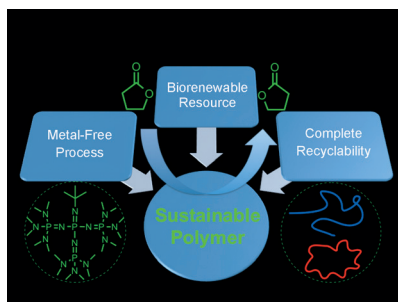


Sustainable Polymers

M. Hong, E. Y.-X. Chen* _____ 4188–4193



Towards Truly Sustainable Polymers:
A Metal-Free Recyclable Polyester
from Biorenewable Non-Strained
 γ -Butyrolactone



Recyclable and renewable: The fast organopolymerization of the biorenewable non-strained γ -butyrolactone has led to a high-molecular-weight metal-free polyester with complete recyclability. The monomer has been long believed to be a non-polymerizable monomer because of its stable five-membered ring structure.

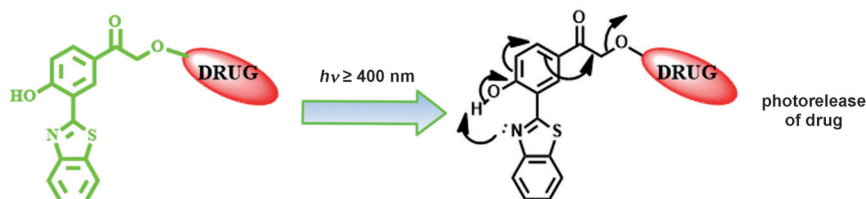
Frontispiece

For the USA and Canada:

ANGEWANDTE CHEMIE International
Edition (ISSN 1433-7851) is published weekly
by Wiley-VCH, PO Box 101161, 69451 Wein-
heim, Germany. US mailing agent: SPP, PO Box
437, Emigsville, PA 17318. Periodicals postage

paid at Emigsville, PA. US POSTMASTER: send
address changes to *Angewandte Chemie*, John
Wiley & Sons Inc., C/O The Sheridan Press, PO
Box 465, Hanover, PA 17331. Annual subscrip-
tion price for institutions: US\$ 16.862/14.051
(valid for print and electronic / print or

electronic delivery); for individuals who are
personal members of a national chemical
society prices are available on request. Postage
and handling charges included. All prices are
subject to local VAT/sales tax.



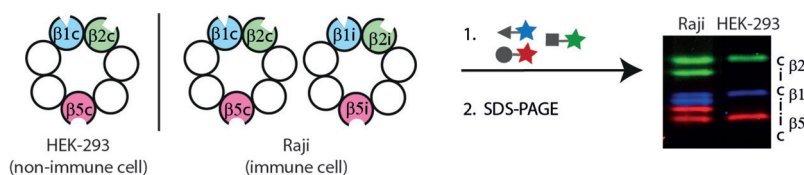
Let it go... The two major limitations for theranostics of the *p*-hydroxyphenacyl (pHP) phototrigger were overcome by incorporating a benzothiazole appendage to enable rapid excited-state intramolecular proton transfer (ESIPT; see picture).

The ESIPT effect had two key advantages: It assisted the deprotonation of pHP group for faster release of the anticancer drug chlorambucil and led to a fluorescence color change upon photorelease.

Photoregulated Drug Release

S. Barman, S. K. Mukhopadhyay, S. Biswas, S. Nandi, M. Gangopadhyay, S. Dey,* A. Anoop,*
N. D. P. Singh* _____ 4194–4198

A *p*-Hydroxyphenacyl–Benzothiazole–Chlorambucil Conjugate as a Real-Time-Monitoring Drug-Delivery System Assisted by Excited-State Intramolecular Proton Transfer



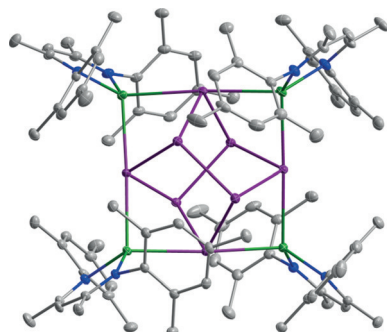
A cocktail of activity-based probes enables the visualization and relative quantification of the six catalytically active subunits of the constitutive proteasome and the immunoproteasome. Proteasome inhibitors were thus characterized, and specific

inhibitors for each subunit were developed. Specific inhibition of the immunoproteasome subunits β5i and β1i proved to be cytotoxic to primary cells from acute lymphocytic leukemia patients.

Activity-Based Protein Profiling

G. de Bruin, B. T. Xin, M. Kraus, M. van der Stelt, G. A. van der Marel, A. F. Kisselev, C. Driessen, B. I. Florea,*
H. S. Overkleeft* _____ 4199–4203

A Set of Activity-Based Probes to Visualize Human (Immuno)proteasome Activities



Reduction reactions of distibines Sb_2R_4 ($\text{R} = \text{Me}, \text{Et}$) with monovalent magnesium complexes $[(\text{L}^{1,2}\text{Mg})_2]$ yielded the first tetraanionic polystibides $[(\text{L}^{1,2}\text{Mg})_4\text{Sb}_8]$ ($\text{L}^1 = \text{HC}[\text{C}(\text{Me})\text{N}(2,4,6\text{-Me}_3\text{C}_6\text{H}_2)]_2$, $\text{L}^2 = \text{HC}[\text{C}(\text{Me})\text{N}(2,6\text{-iPr}_2\text{C}_6\text{H}_3)]_2$), in which the central Sb_8 cores adopt realgar-type structures. Atom colors: Mg = green; Sb = purple; N = blue; C = gray.

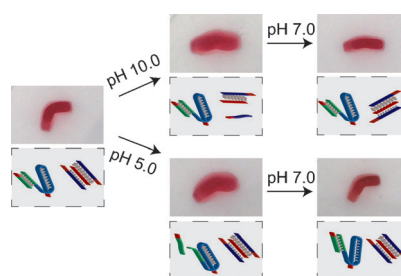
Polystibides

C. Ganesamoorthy, C. Wölper, A. S. Nizovtsev, S. Schulz* _____ 4204–4209

Synthesis and Structural Characterization of Magnesium-Substituted Polystibides $[(\text{LMg})_4\text{Sb}_8]$



An acrylamide–DNA hydrogel of a defined shape has been synthesized by crosslinking the polymer chains with two different pH-responsive oligonucleotide units. The hydrogel was transformed into a soft, shapeless state by a pH-induced selective dissociation of one of the crosslinker types, while the second crosslinking unit was retained as internal memory.



DNA Nanostructures

Y. Hu, W. Guo, J. S. Kahn, M. A. Aleman-Garcia, I. Willner* _____ 4210–4214

A Shape-Memory DNA-Based Hydrogel Exhibiting Two Internal Memories

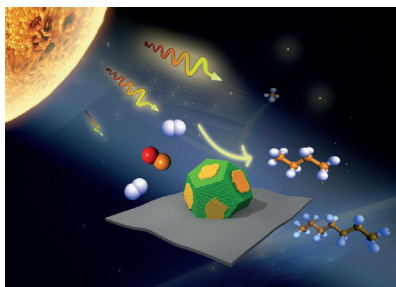


**Photocatalysis**

Y. Zhao, B. Zhao, J. Liu, G. Chen, R. Gao, S. Yao, M. Li, Q. Zhang, L. Gu, J. Xie, X. Wen,* L.-Z. Wu, C.-H. Tung, D. Ma,* T. Zhang* ————— **4215–4219**



Oxide-Modified Nickel Photocatalysts for the Production of Hydrocarbons in Visible Light



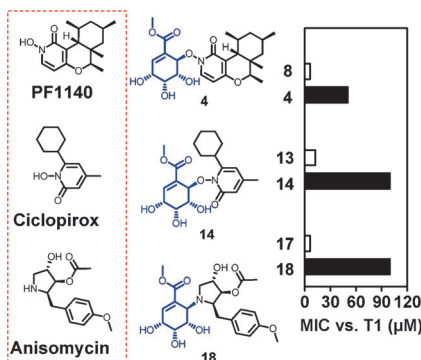
Production of hydrocarbons: Oxide-decorated metal nickel nanoparticle catalysts were prepared and used for the photocatalytic hydrogenation of carbon monoxide to C_{2+} hydrocarbons in visible light. The work highlights the possibility of using solar energy to produce fuels and chemicals under mild reaction conditions.

Natural Products

L. Du, J. You, K. M. Nicholas, R. H. Cichewicz* ————— **4220–4225**



Chemoreactive Natural Products that Afford Resistance Against Disparate Antibiotics and Toxins



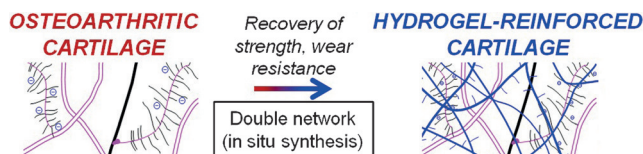
Electrophilic warheads: Fungus-derived shikimate analogues, pericoside and pericosine A (see picture; blue), have been identified as archetypal chemoreactive natural products that neutralize the antagonistic properties of chemically diverse synthetic and naturally derived antifungal agents and toxins (see picture; left).

**Biomaterials**

B. G. Cooper, R. C. Stewart, D. Burstein, B. D. Snyder, M. W. Grinstaff* ————— **4226–4230**



A Tissue-Penetrating Double Network Restores the Mechanical Properties of Degenerated Articular Cartilage



Bring in the reinforcements: Softened and wear-prone articular cartilage is reinforced by a semi-natural–semi-synthetic interpenetrating polymer network. In situ photopolymerization of biomimetic mon-

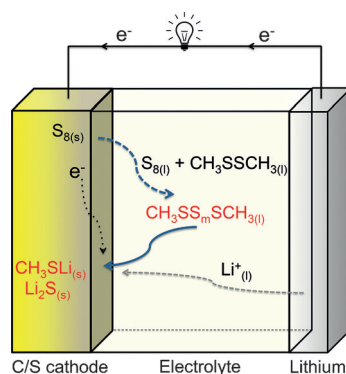
omers within the tissue increases cartilage strength and wear-resistance. This biomaterials-based approach may hold promise for treating early stage osteoarthritis.

Batteries

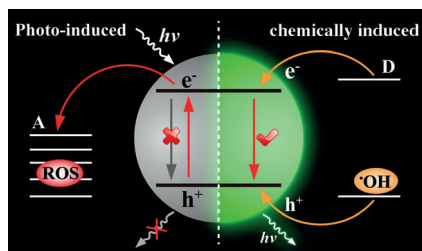
S. Chen, F. Dai, M. L. Gordin, Z. Yu, Y. Gao, J. Song, D. Wang* — **4231–4235**



Functional Organosulfide Electrolyte Promotes an Alternate Reaction Pathway to Achieve High Performance in Lithium–Sulfur Batteries



Finding the right electrolyte: Dimethyl disulfide (DMDS) was reported as a functional co-solvent for Li–S electrolytes. DMDS enabled an alternative discharge pathway for sulfur cathodes by formation and subsequent reduction of dimethyl polysulfide (DMPS) intermediates, showing a much higher capacity and more stable cycling performance than that of conventional Li–S cells.

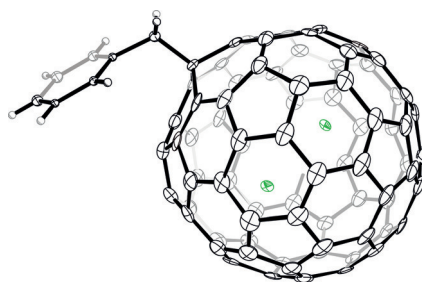


HO[•] selective: A novel quantum dot (QD) based turn-on luminescent probe for the specific detection of hydroxyl radicals was designed and used for monitoring the endogenous release of such species in living cells. Metal citrate complexes on the surfaces of the QDs play a crucial role as electron donors. Importantly, this luminescent probe does not respond to other reactive oxygen species (ROS).

Luminescent Probes

W. J. Zhou, Y. Q. Cao, D. D. Sui, C. Lu* — 4236 – 4241

Turn-On Luminescent Probes for the Real-Time Monitoring of Endogenous Hydroxyl Radicals in Living Cells



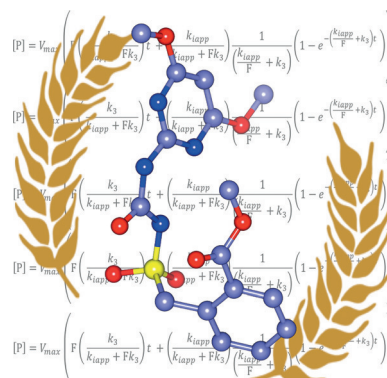
A stable fullerene radical La₂@I_h-C₈₀(C₇H₇) was synthesized and fully characterized. The stability of the radical is attributed to the localization of the unpaired electron inside the cage, as suggested by EPR spectroscopy and DFT calculations. Metal–metal bonding is indicated by the La–La distance, which is consistent with the calculated distance, and the localization of the SOMO on the La₂ unit.

Fullerene Radicals

L. Bao, M. Chen, C. Pan, T. Yamaguchi, T. Kato, M. M. Olmstead, A. L. Balch, T. Akasaka, X. Lu* — 4242 – 4246

Crystallographic Evidence for Direct Metal–Metal Bonding in a Stable Open-Shell La₂@I_h-C₈₀ Derivative

How AHAS-inhibiting herbicides work: Acetohydroxyacid synthase (AHAS) inhibitors, such as bensulfuron methyl (see picture), are successful commercial herbicides; however, their mechanism of inhibition is poorly understood. To address this issue, a new equation is proposed that both accounts for the accumulative and reversible inhibition of AHAS and explains all previous experimental data. Atom colors: C = blue; N = dark blue; O = red; S = yellow.

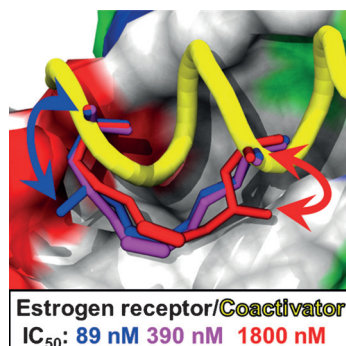


Enzyme Kinetics

T. Lonhienne,* A. Nouwens, C. M. Williams, J. A. Fraser, Y. Lee, N. P. West, L. W. Guddat* — 4247 – 4251

Commercial Herbicides Can Trigger the Oxidative Inactivation of Acetohydroxyacid Synthase

Branching out: γ -Branched stapling amino acids were synthesized and incorporated into peptides to produce high-affinity inhibitors of the estrogen receptor/steroid receptor coactivator interaction. Some branched stapled peptides were more effective than the unfunctionalized peptide. The influence of 1,5-interactions on peptide conformation was analyzed by circular dichroism, X-ray crystallography, and molecular dynamics.



Peptidomimetics

T. E. Speltz, S. W. Fanning, C. G. Mayne, C. Fowler, E. Tajkhorshid, G. L. Greene, T. W. Moore* — 4252 – 4255

Stapled Peptides with γ -Methylated Hydrocarbon Chains for the Estrogen Receptor/Coactivator Interaction

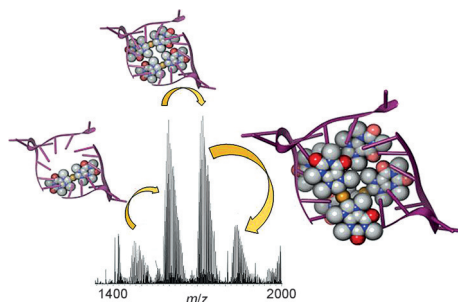
Inside Cover

Anticancer Agents

C. Bazzicalupi, M. Ferraroni,* F. Papi,
L. Massai, B. Bertrand, L. Messori,
P. Gratteri,* A. Casini — 4256–4259



Determinants for Tight and Selective Binding of a Medicinal Dicarbene Gold(I) Complex to a Telomeric DNA G-Quadruplex: a Joint ESI MS and XRD Investigation



Ready for takeoff: A crystal structure analysis of the adduct formed between $[\text{Au}(\text{9-methylcaffeine-8-ylidene})_2]^+$ and Tel 23 DNA G-quadruplex is presented. In the

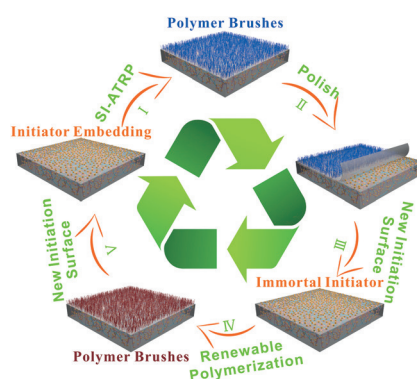
adduct, Tel 23 maintains a characteristic propeller conformation, while binding three gold(I) dicarbene moieties at two distinct sites.

Surface Modifications

T. Du, B. Li, X. Wang, B. Yu, X. Pei,
W. T. S. Huck, F. Zhou* — 4260–4264



Bio-Inspired Renewable Surface-Initiated Polymerization from Permanently Embedded Initiators



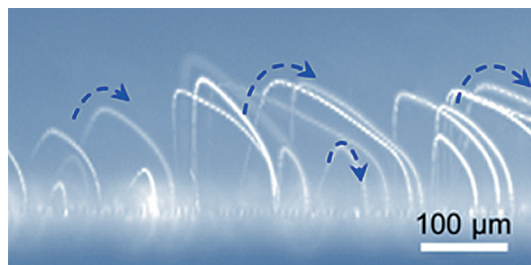
A simple and robust method is reported to repeatedly modify surfaces with polymer brushes through SI-ATRP, based on an initiator-embedded polystyrene sheet. This method outpaces traditional surface grafting technologies owing to unlimited grafting cycles, and it can be combined with carving, micromachining, and hot embossing, and allows stereoselective polymer grafting and metal deposition.

Superhydrophobic Surfaces

J. Liu, H. Guo, B. Zhang, S. Qiao, M. Shao,
X. Zhang, X. Feng, Q. Li,* Y. Song, L. Jiang,
J. Wang* — 4265–4269



Guided Self-Propelled Leaping of Droplets on a Micro-Anisotropic Superhydrophobic Surface



Jumping Jack Flash: Water microdroplets can coalesce and leap over the surface spontaneously along a prescribed direction upon introducing anisotropic micro-patterns onto superhydrophobic surfaces.

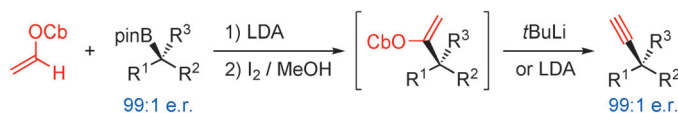
These surfaces offer efficient self-powered and relatively long-distance transport of microdroplets by “relay” coalescence-induced leaping and effective self-sustained microcarriers.

Boronic Ester Reactions

Y. Wang, A. Noble, E. L. Myers,
V. K. Aggarwal* — 4270–4274

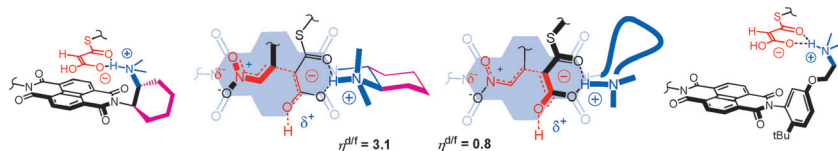


Enantiospecific Alkynylation of Alkylboronic Esters



Enantiospecific alkynylation: Enantioenriched secondary and tertiary alkyl pinacolboronic esters undergo enantiospecific deborylative alkynylation through a Zwei-

fel-type alkenylation followed by a 1,2-elimination reaction to give alkynes in high yield and essentially complete enantiospecificity.



Served on a platter: Simple, compact, and precisely sculpted Leonard turns are introduced to firmly and reliably place reactions on aromatic surfaces, minimizing entropic costs to maximize enthalpic gains. The significant change in selectivity

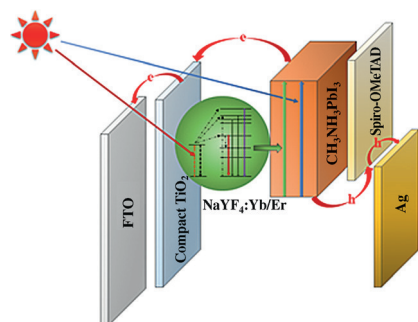
($r^{d/f}$) from less desirable decarboxylation with loose turns (right) to more relevant enolate addition pathways on π -acidic surfaces with rigidified Leonard turns (left) demonstrates the power of this concept.

Preorganization



Y. Cotellet, S. Benz, A.-J. Avestro,
T. R. Ward, N. Sakai,
S. Matile* ————— 4275 – 4279

Anion- π Catalysis of Enolate Chemistry:
Rigidified Leonard Turns as a General
Motif to Run Reactions on Aromatic
Surfaces



A strategy for integrating NaYF₄:Yb/Er upconversion nanoparticles as a mesoporous electrode into CH₃NH₃PbI₃ perovskite solar cells makes it possible to operate the cells with near-infrared light. The in situ integration of upconversion materials as functional components in perovskite solar cells offers flexibility for engineering the device architecture and broadening the use of solar radiation.

Photovoltaic Devices

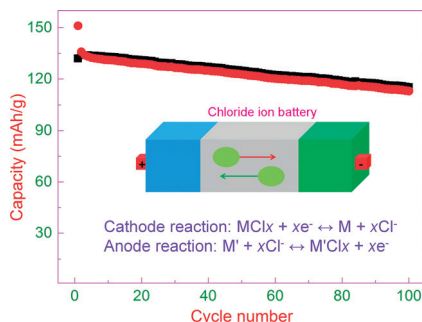


M. He, X. Pang, X. Liu, B. Jiang, Y. He,
H. Snaith, Z. Lin* ————— 4280 – 4284

Monodisperse Dual-Functional
Upconversion Nanoparticles Enabled
Near-Infrared Organolead Halide
Perovskite Solar Cells



Inside Back Cover

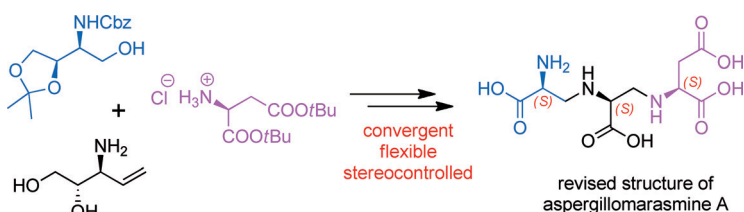


Chloride shuttle: A rechargeable chloride ion battery is based on the reversible transfer of chloride ions between a VOCl cathode and lithium anode. A reversible capacity of 113 mAh g⁻¹ can be retained after 100 cycles even at a high current density rating of 2 C. Key: ● Cl⁻, ■ MCl_x (cathode), ■ M' (anode), → discharging, ← charging.

Rechargeable Batteries

P. Gao, M. A. Reddy, X. Mu, T. Diemant,
L. Zhang, Z. Zhao-Karger,
V. S. K. Chakravadhanula, O. Clemens,
R. J. Behm, M. Fichtner* — 4285 – 4290

VOCl as a Cathode for Rechargeable
Chloride Ion Batteries



Resistance is futile: The natural product aspergillomarasmine A (AMA) is a potent inhibitor of metallo- β -lactamase-1, which mediates resistance to β -lactam antibiotics. The presented total synthesis of AMA allowed a reassignment of its stereo-

chemical configuration. The synthetic route is amenable to the efficient preparation of analogues for the development of potent and selective metallo- β -lactamase inhibitors.

Antibiotics

D. Liao, S. Yang, J. Wang, J. Zhang,
B. Hong, F. Wu, X. Lei* — 4291 – 4295

Total Synthesis and Structural
Reassignment of Aspergillomarasmine A



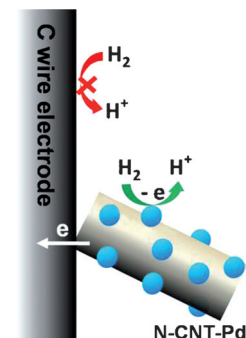
**Electrochemistry**

X. Li, C. Batchelor-McAuley,
S. A. I. Whitby, K. Tschulik, L. Shao,
R. G. Compton* ————— **4296–4299**



Single Nanoparticle Voltammetry:
Contact Modulation of the Mediated
Current

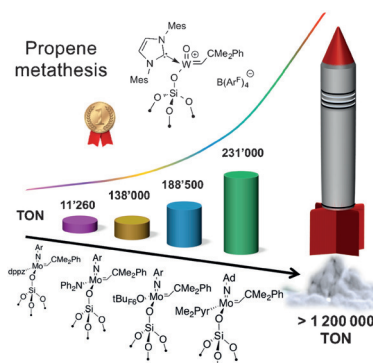
Catalysis at the nanoscale: The cyclic voltammetric responses of individual palladium-coated nitrogen-doped multi-walled carbon nanotubes (N-CNT-Pd; see picture) were studied. The nanoparticles acted as individual nanoelectrodes that catalyzed the hydrogen-oxidation reaction.

**Supported Catalysts**

M. Pucino, V. Mougel, R. Schowner,
A. Fedorov, M. R. Buchmeiser,*
C. Copéret* ————— **4300–4302**



Cationic Silica-Supported N-Heterocyclic
Carbene Tungsten Oxo Alkylidene Sites:
Highly Active and Stable Catalysts for
Olefin Metathesis



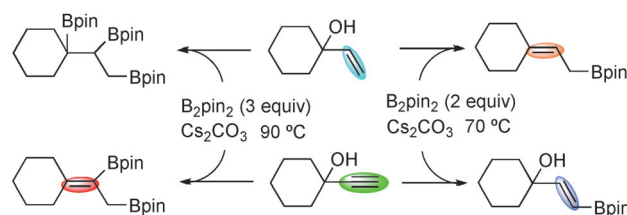
Like a rocket: A well-defined silica-supported cationic N-heterocyclic carbene tungsten oxo alkylidene catalyst $(B(Ar^F)_4 = B(3,5-(CF_3)_2C_6H_3)_4$, Mes = mesityl) was synthesized and fully characterized by elemental analysis, infrared spectroscopy, and solid-state NMR spectroscopy. The catalyst demonstrated very high activity for the metathesis of olefins.

Borylation

N. Miralles, R. Alam, K. J. Szabó,*
E. Fernández* ————— **4303–4307**



Transition-Metal-Free Borylation of Allylic
and Propargylic Alcohols



A transition-metal-free allylic borylation of tertiary allylic alcohols provides access to new allylic boronates. The reactions were carried out in the presence of 15 mol % of CS_2CO_3 and MeOH to promote the Lewis

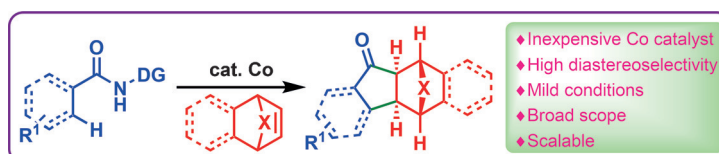
acid–base adduct formation $[Hbase]^+[MeO-B_2pin_2]^-$, which may be responsible for generating unprecedented 1,2,3-polyborylated products.

C–H Activation

P. Gandeepan, P. Rajamalli,
C.-H. Cheng* ————— **4308–4311**



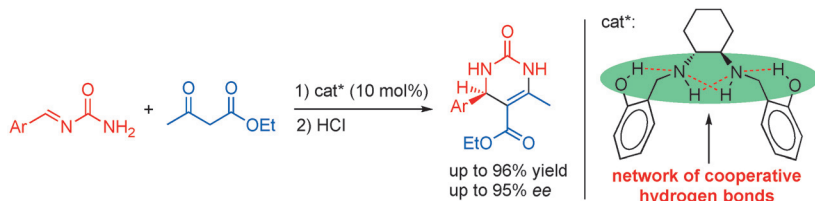
Diastereoselective [3+2] Annulation of
Aromatic/Vinyl Amides with Bicyclic
Alkenes through Cobalt-Catalyzed C–H
Activation and Intramolecular
Nucleophilic Addition



[3+2] instead of [4+2] or [4+1]: The diastereoselective [3+2] annulation of secondary amides with alkenes proceeds by cobalt-catalyzed C–H activation and intramolecular nucleophilic addition to

the amide functional group under mild conditions. Mechanistic studies suggest that the C–H bond cleavage is the rate-limiting step.

Back Cover



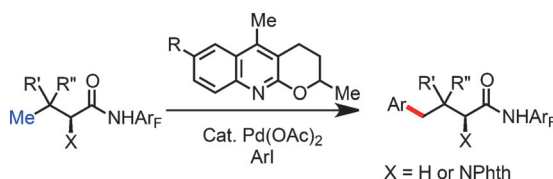
Caught in the net: The standard roles that the actors (nucleophile, electrophile, and catalyst) perform during the catalytic act in the arena of bifunctional catalysis were switched in the search for bioinspired organocatalysts. It was thus found that

the network of hydrogen bonds provided by salan derivatives catalyzed the Mannich reaction of arylideneureas with acetates in an enantioselective, biomimetic manner (see scheme).

Asymmetric Catalysis

V. J. Lillo, J. Mansilla,
J. M. Saá* 4312–4316

Organocatalysis by Networks of Cooperative Hydrogen Bonds: Enantioselective Direct Mannich Addition to Preformed Arylideneureas



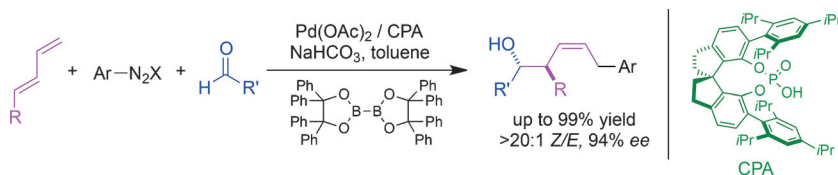
Pd^{II}-catalyzed arylation of γ -C(sp³)-H bonds of aliphatic acid-derived amides was developed by using quinoline-based ligands. Various γ -aryl- α -amino acids were

prepared from natural amino acids using this method. The influence of ligand structure on reactivity was also systematically investigated.

C–H Activation

S. Li, R.-Y. Zhu, K.-J. Xiao,
J.-Q. Yu* 4317–4321

Ligand-Enabled Arylation of γ -C–H Bonds



Catalysis combo: A highly selective multicomponent carbonyl allylation reaction of 1,3-butadienes, aryldiazonium tetrafluoroborates, and aldehydes has been established under combined palladium

acetate and chiral anion phase-transfer catalysis. The protocol leads to the assembly of chiral Z-configured homoallylic alcohols in high yields and with excellent levels of enantioselectivity.

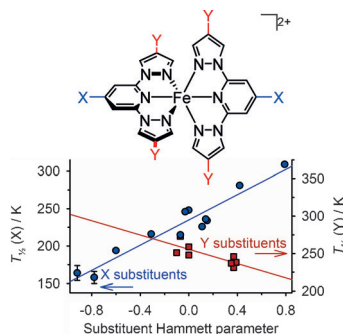
Asymmetric Catalysis

Z.-L. Tao, A. Adili, H.-C. Shen, Z.-Y. Han,
L.-Z. Gong* 4322–4326

Catalytic Enantioselective Assembly of Homoallylic Alcohols from Dienes, Aryldiazonium Salts, and Aldehydes



Highs and lows: The low-spin state of the complex shown is stabilized by electron-withdrawing pyridyl “X” substituents, but also by electron-donating pyrazolyl “Y” substituents. DFT calculations reproduce these results, which arise from competing influences of pyridyl and pyrazolyl ligand substituents on Fe–L σ and π bonding.



Spin State

L. J. Kershaw Cook, R. Kulmaczewski,
R. Mohammed, S. Dudley, S. A. Barrett,
M. A. Little, R. J. Deeth,*
M. A. Halcrow* 4327–4331

A Unified Treatment of the Relationship Between Ligand Substituents and Spin State in a Family of Iron(II) Complexes

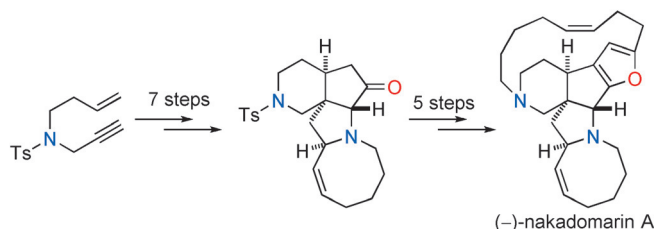


Marine Alkaloids

J. S. Clark,* C. Xu — 4332–4335



Total Synthesis of (–)-Nakadomarin A



The later the better: A highly efficient 12-step synthesis of (–)-nakadomarin A is reported. The key tetracyclic ketone intermediate was constructed from a simple enyne in seven steps. As the furan is

introduced at a later synthetic stage, this intermediate may have potential in the syntheses of related marine alkaloids such as manzamine A and ircinal A.

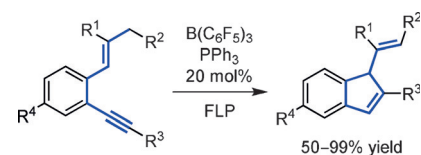
FLP Catalysis

S. Tamke, Z.-W. Qu, N. A. Sitte, U. Flörke, S. Grimme,* J. Paradies* — 4336–4339



Frustrated Lewis Pair-Catalyzed Cycloisomerization of 1,5-Enynes via a 5-*endo*-dig Cyclization/Protodeborylation Sequence

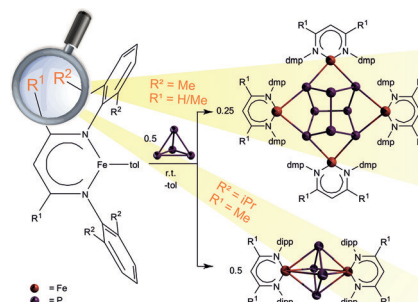
Cycloisomerization without a metal: The first FLP-catalyzed C–C bond forming reaction is described as proceeding through a cycloisomerization/protodeborylation sequence. The reaction mechanism is supported by X-ray crystal structure analysis of intermediates, kinetic experiments, and by quantum-mechanical calculations.

P₄ Activation

F. Spitzer, C. Graßl, G. Balázs, E. M. Zolnhofer, K. Meyer, M. Scheer* — 4340–4344



Influence of the nacnac Ligand in Iron(I)-Mediated P₄ Transformations



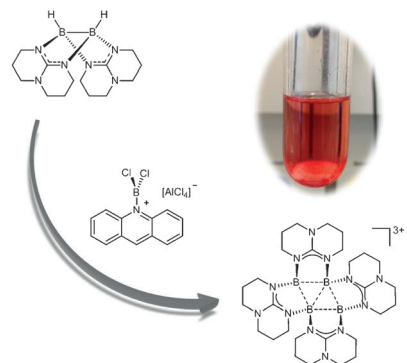
Depending on the size of the substituents of the *N,N'*-diarylated β-diketiminato ligands, iron(I) complexes activate white phosphorus in different ways. Small substituents result in dimerization with formation of a realgar-like P₈ ligand at the center of a tetranuclear complex; larger substituents lead to planarization in dinuclear *cyclo*-P₄ complexes.

Boron Compounds

S. Litters, E. Kaifer, H.-J. Himmel* — 4345–4347

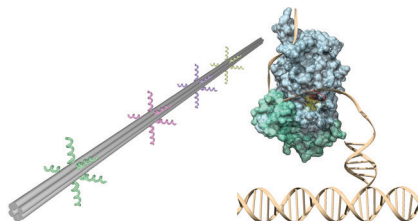


A Radical Tricationic Rhomboid Tetraborane(4) with Four-Center, Five-Electron Bonding



Share and share alike: Reaction of the doubly base-stabilized diborane(4) [HB(hpp)₂]₂ with the strong hydride abstraction reagent [(acridine)BCl₂][AlCl₄] leads to the unprecedented red-colored tetraborane(4) [B₄(hpp)₄]³⁺ with a rhomboid B₄ skeleton and four-center, five-electron bonding.

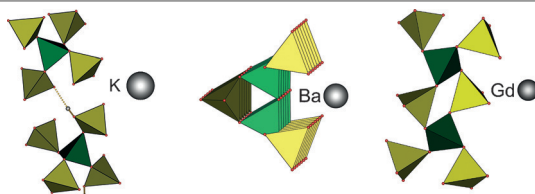
In nature, relaxase proteins are involved in the conjugative transfer of plasmids between bacteria. Here it is shown that their specificity for a single-stranded DNA target, their good orthogonality, and their binding properties can also be utilized for the functionalization of DNA nanostructures with proteins.



DNA Nanotechnology

S. Sagredo, T. Pirzer, A. Aghebat Rafat, M. A. Goetzfried, G. Moncalian, F. C. Simmel,*
F. de la Cruz* _____ 4348–4352

Orthogonal Protein Assembly on DNA Nanostructures Using Relaxases



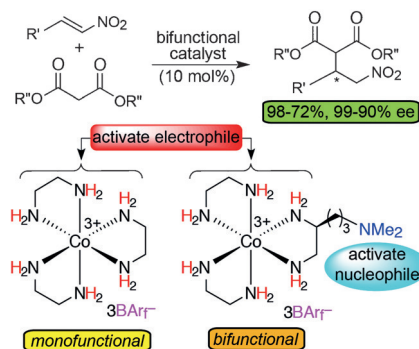
Extension of structural variability is the feature of the first borosulfates of a divalent and a trivalent cation showing band-silicate (see picture; middle: borate tetrahedra green, sulfate tetrahedra yellow)

and cyclosilicate topologies (right), which were obtained by a new synthetic approach. Moreover, the first hydrogen-borosulfate is presented (left; small spheres: H).

Borosulfates

P. Gross, A. Kirchhain, H. A. Höppe* _____ 4353–4355

The Borosulfates $K_4[BS_4O_{15}(OH)]$, $Ba[B_2S_3O_{13}]$, and $Gd_2[B_2S_6O_{24}]$

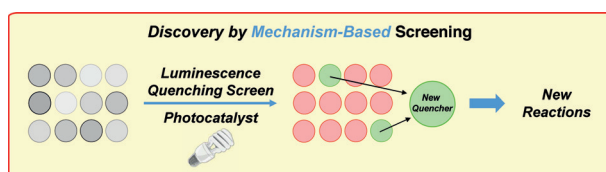


Two are better than one: Unlike the catalyst $\Lambda\text{-}[\text{Co}(\text{en})_3]^{3+} 3 \text{BARf}^-$, the bifunctional tertiary-amine-containing analogue $\Lambda\text{-}3\text{c}^{3+} 3 \text{BARf}^-$ effects highly enantioselective additions of alkyl malonates to β -aryl- and β -alkylnitroethenes. The efficacy diminishes as the $(\text{CH}_2)_3$ tether is shortened or lengthened.

Bifunctional Catalysts

S. K. Ghosh, C. Ganzmann, N. Bhuvanesh, J. A. Gladysz* _____ 4356–4360

Werner Complexes with ω -Dimethylaminoalkyl Substituted Ethylenediamine Ligands: Bifunctional Hydrogen-Bond-Donor Catalysts for Highly Enantioselective Michael Additions



Enlightened! A mechanism-based screening approach can accelerate discovery in photocatalysis. It focuses on a single mechanistic step of a reaction class: the quenching step central to photocatalytic transformations. Luminescence spectroscopy

was used to screen 100 compounds, identifying two promising substrate classes. A second, more-focused screen provided mechanistic insights for developing proof-of-concept reactions.

Screening Methods

M. N. Hopkinson, A. Gómez-Suárez, M. Teders, B. Sahoo, F. Glorius* _____ 4361–4366

Accelerated Discovery in Photocatalysis using a Mechanism-Based Screening Method

Front Cover



Supporting information is available on www.angewandte.org (see article for access details).



A video clip is available as Supporting Information on www.angewandte.org (see article for access details).



This article is available online free of charge (Open Access).



This article is accompanied by a cover picture (front or back cover, and inside or outside).



The Very Important Papers, marked VIP, have been rated unanimously as very important by the referees.



The Hot Papers are articles that the Editors have chosen on the basis of the referee reports to be of particular importance for an intensely studied area of research.